Current Optics and Photonics

Regular Paper

Waveguide-type Multidirectional Light Field Display

Hyungju Rah, Seungmin Lee, Yeong Hwa Ryu, Gayeon Park, and Seok Ho Song*

Department of Physics, Hanyang University, Seoul 04763, Korea

We demonstrate two types of light field displays based on waveguide grating coupler arrays: a line beam type and a point source type. Ultra violet imprinting of an array of diffractive nanograting cells on the top surface of a 50-μm-thin slab waveguide can deliver a line beam or a point beam to a multidirectional light field out of the waveguide slab. By controlling the grating vectors of the nanograting cells, the waveguide modes are externally coupled to specific viewing angles to create a multidirectional light field display. Nanograting cells with periods of 300 nm–518 nm and slanted angles of −8.5°~+8.5° are fabricated by two-beam interference lithography on a 40 mm × 40 mm slab waveguide for seven different viewpoints. It is expected that it will be possible to realize a very thin and flexible panel that shows multidirectional light field images through the waveguide-type diffraction display.

Keywords : 3D display, Grating diffraction efficiency, Light field display
OCIS codes : (050.1950) Diffraction gratings; (110.4190) Multiple imaging

I. INTRODUCTION

There are several techniques to provide different information to each eye by forming binocular disparity using eyeglasses, lenticular lenses, or parallax barriers [1]. AR glasses technology, which uses transparent displays to enable interaction between the information projected on a screen and the visible outside world, is also making great strides [2]. The development of a display system with thinner, transparent, and flexible characteristics has recently opened up the possibility of next-generation displays in the form of head mounts [3], glasses [4], and contact lenses [5]. It can be said that one of optical key elements required for next-generation 3D display depends on how a multidirectional display system can be implemented in a compact and integrated format with low cross-talk. To accomplish this requirement, very thin and multifunctional optical elements such as binary optics [6, 7], computer-generated holograms [8], diffractive waveguides [9–11], embedded beam splitters [12], and meta-surface optics [13] are being developed. In particular, the diffractive waveguide-type display based on nanograting cell arrays is attracting considerable attention as a technology suitable for a light field display method that allows a 3D image to be viewed by dispersing an input pattern to various viewing directions [14–18].

In this paper, we demonstrate two types of light field displays using a diffractive waveguide approach. One is designed to focus line-shaped incident light on one edge of the diffractive waveguide, and the other is a waveguide branching structure that transmits a point-shaped light source incident on the diffractive waveguide as a line beam. Both form various viewing angles by transmitting an incident beam in waveguide mode to a diffraction grating cell by a nanograting cell array formed on a multimode waveguide. The nanograting cells are designed to diffract a guided mode at a specific altitude and azimuth angle with period range from 300 nm to 518 nm. The waveguide is fabricated to a thickness of 50 μm on a Si wafer by spin-coating and curing the cladding and core materials, and the diffractive nanograting cells are fabricated using two-beam interference lithography and the ultra violet (UV) imprinting process. The measurement results of seven viewpoint

---

*Corresponding author: shsong@hanyang.ac.kr, ORCID 0000-0002-1777-6169

Color versions of one or more of the figures in this paper are available online.

− 375 −

images obtained from the two-types of diffractive waveguides reveal a possibility to implement a very thin and compact panel for multidirectional light field display.

II. DESIGN AND FABRICATION

The structure of the diffractive waveguide demonstrated here is shown in Fig. 1(a). A guiding mode coupled from a light source propagates through the waveguide core before out-coupling to multidirectional light fields from an array of diffraction grating cells. The core and cladding layers are made using a bottom-up process as shown in Fig. 1(b). A 20-μm-thick cladding material [n = 1.47, tetra (ethylene glycol) diacrylate; Sigma Aldrich, MO, USA] is spin-coated on a clean silicon substrate, and cured with a UV lamp (365 nm in wavelength, 20 mW/cm^2). A core (15-μm-thick) material (n = 1.5, Bisophenol A ethoxylate diacrylate; Sigma Aldrich) is then spin-coated on the cladding layer and cured with the same UV lamp. A photoresist layer (AZ5206; MicroChemicals, Ulm, Germany) on a different substrate is used for the lithography material of a two-beam interference system (351 nm in wavelength) as shown in Fig. 1(c) to form 10-μm-square grating cells, with periods of 300

nm–1,000 nm and slanted angles of 0°–180° as shown in Fig. 1(d). Finally, the photoresist grating layer is transferred to the core layer by UV imprinting.

After a numerical calculation, the number of modes coupled in the diffractive waveguide was found to be about 19 for a 532 nm incident beam (COMSOL Multi Physics; COMSOL, MA, USA). The effective indices of the coupled modes give us the incidence angles to the grating cells, distributed between 75° and 89° from normal direction. An average angle of 82° is used for demonstrating the two types of multi-view display system. The modulation depth of the gratings imprinted on the waveguide core is 120 nm, resulting in an overall out-coupling efficiency of 22.9% after propagating a 40-mm-long diffractive waveguide.

III. RESULTS

3.1. Line Beam Type Diffractive Waveguide Display

Figures 2(a) and 2(b) show schematics of the line beam type diffractive waveguide. An incident beam from an optical fiber is converted to a line beam focused to the waveguide core after transmitting an engineered diffuser (ED 1-L4100; Thorlabs, NJ, USA) and a pair of cylindrical lens-
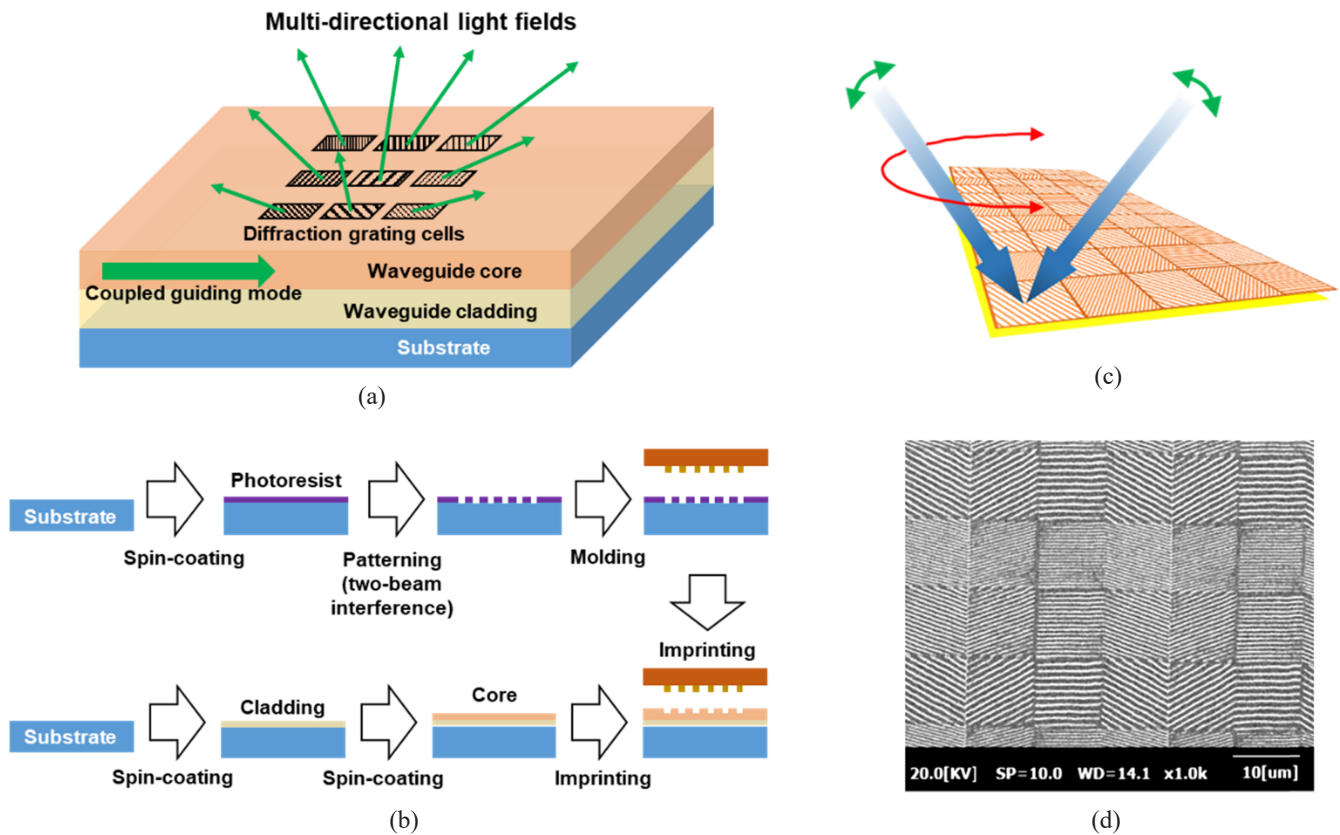

(a)

(c)

(b)

(d)

FIG. 1. Structure of a diffractive waveguide-type panel. (a) Schematic diagram of diffractive waveguides for a light field display. A coupled guiding mode propagates along the waveguide core before out-coupling to multiple directions from an array of diffraction grating cells. (b) Fabrication process of the diffractive waveguide-type panel by ultra violet (UV) imprinting via two-beam interference in (c). Two square-aperture beams interfere with various vertical (green arrows) and azimuthal (red) angles, resulting in a grating cell array with different periods and grating directions. (d) Scanning electronic microscope (SEM) images of a typical fabricated grating array of 10-μm-square cells.
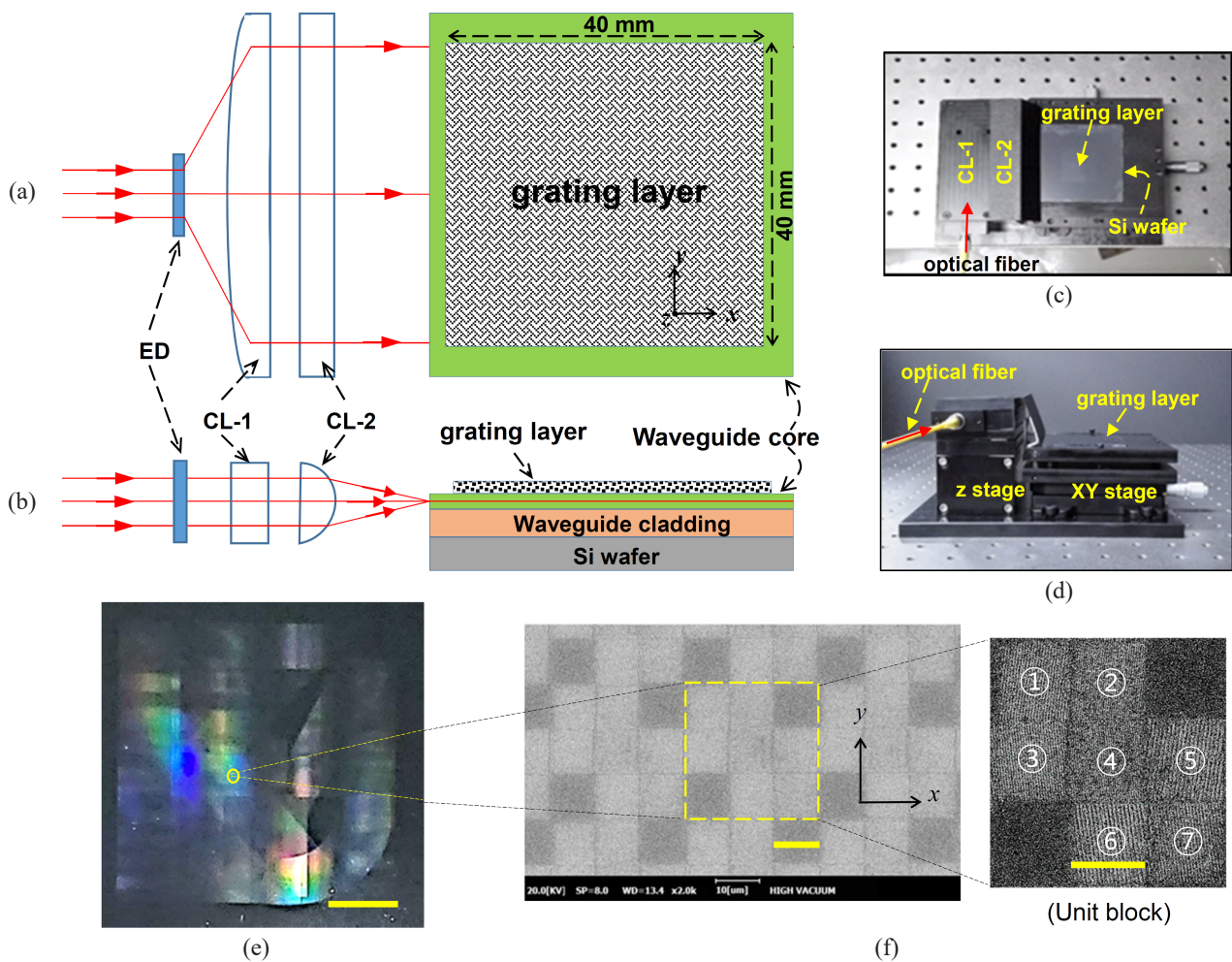
FIG. 2. Line beam type setup for diffractive waveguide display. (a, b) Schematic diagrams of the line beam type diffractive waveguide system. ED, engineered diffuser; CL-1, cylindrical lenses; CL-2, half-dome rod lenses. (c) Top view and (d) side view of the experiment setup. An optical fiber is used for incident light and an XYZ stage for alignment between the focused line beam and the waveguide core. (e) and (f) Photographs of the fabricated grating layer imprinted on the waveguide core. The periods and slanted angles of the seven grating cells, denoted by ①–⑦ in (f), are the range of 300 nm–518 nm and −8.5°~+8.5°, respectively, and two blank cells at the off-diagonal corners. The scale bar in (e) is 10 mm and those in (f) are 10 μm.

es (CL-1, LJ1895L1-A; Thorlabs, NJ, USA) and half-dome lenses made by a fused silica rod. The photos in Fig. 2(c) and 2(d) a show top view and side view of the experimental setup, where an XYZ stage is used for aligning the focused line beam to the core of waveguide. The grating layer of 10 μm-square grating cells are formed on a 40 mm × 40 mm area, composed of (4,000 × 4,000) grating cells in total. If the number of multidirectional light fields is N, the image resolution of each light field is defined by (4,000 × 4,000) / N. For a case when $N = 9$ in the experiment, the grating layer in Fig. 2(e) is composed by an array of unit blocks, and each unit block has (3 × 3) 10 μm-square grating cells as shown in Fig. 2(f). The out-coupling angles from the grating cells are addressed from $\theta = -15°$ to $+30°$ in the horizontal direction while $\Phi = \pm10°$ fixed in the vertical direction. The periods and slanted angles from y-axis of the seven grating cells in the unit block are ① 382 nm, +7.5°; ② 300 nm, +5.4°; ③ 350 nm, −6.5°; ④ 300 nm, −5.4°; ⑤

518 nm, +8.5°; ⑥ 518 nm, −8.5°; and ⑦ 420 nm, −7.6°, and two blank cells at the off-diagonal corners.

Figures 3(a)–3(g) show the seven different images with a resolution of approximately (1,000 × 1,000) pixels measured in each (θ, Φ) direction by using the line beam type diffractive waveguide setup in Fig. 2. The measured images are fairly clear and distinguished. Differences between the designed and measured ones are discussed as follows: First, the tilted images in the experiment are mainly caused by the viewing angle of camera while taking the images. Second, the not-uniform intensity of the experimental images is possibly caused by a rough edge of the cleaved waveguide core layer and not constant out-coupling efficiency of the grating cells. The cleaved edge of the polymeric core and cladding materials are stretched into a rough edge. This could be improved by polishing the coupling edge to make a clean surface. Lastly, the blurred background of the measured images is mainly due to the multiple guiding modes. Each
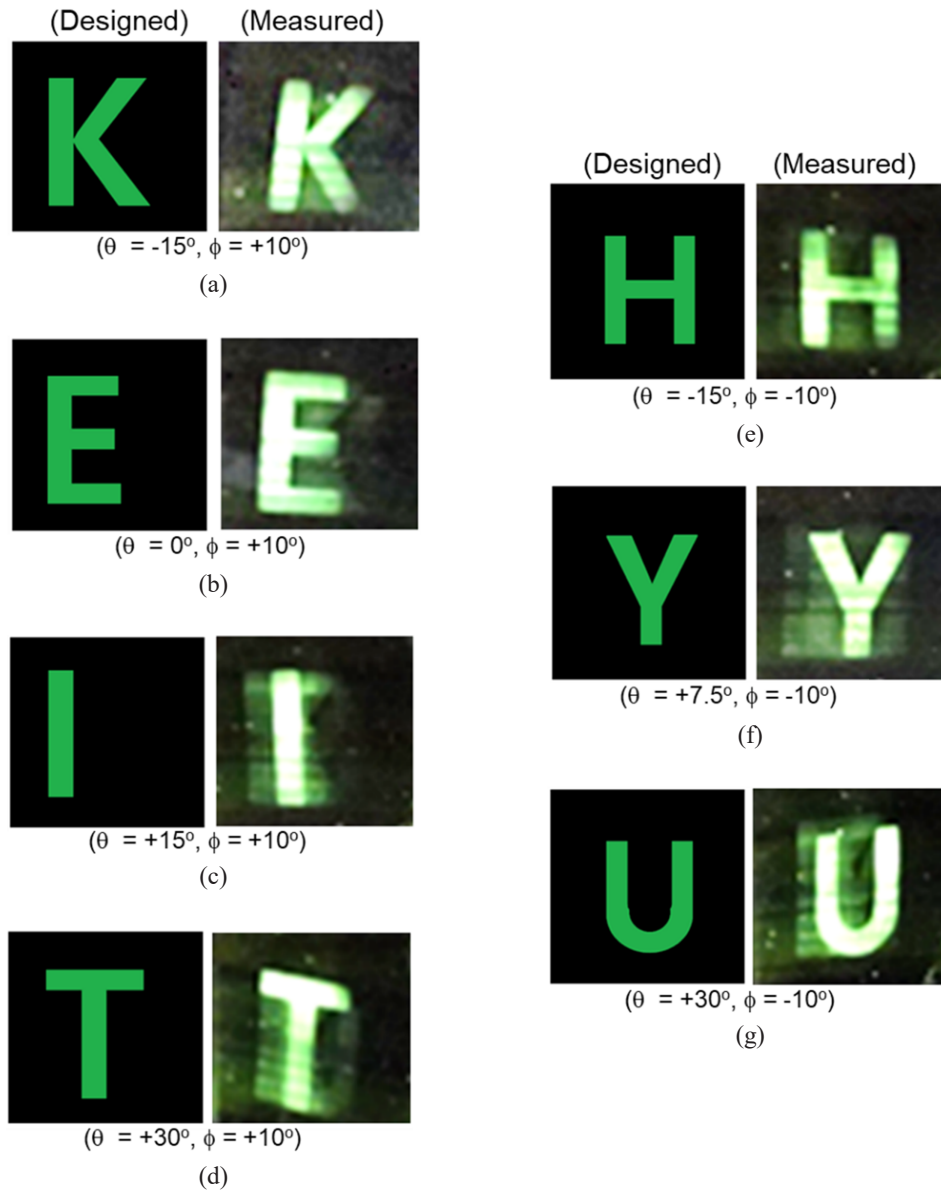
FIG. 3. Designed and measured images of seven viewing angles from the normal direction of the waveguide panel. Each measured image is shown most brightly at the specific viewing angles (θ, ϕ) denoted in (a)–(g) with background noises of weak cross-talk ghost images.

guiding mode causes a different image to be overlapped in blurring. This could be reduced if the thickness of the core layer is reduced to a single mode condition of less than 5 μm.

3.2. Point Source Type Diffractive Waveguide Display

The line beam type showed potential for use in a multidirectional diffractive waveguide display, but the system used to form a line beam was bulky, as a cylindrical lens and rod lens were used to produce a focused line beam coupled to the waveguide. To make it compact, a point source type diffractive waveguide setup was designed and demonstrated as shown in Fig. 4. The schematic in Fig. 4(a) shows the design of a planar structure [19], which is composed of a tapered slab waveguide coupled to an opti-

cal fiber, curved waveguide branches, and a grating layer on top of the (40 mm × 40 mm) planar waveguide area. The input cross-section of the tapered slab waveguide is 2 mm in width and 18 μm in thickness. The 50 curved waveguide branches connected to the 40-mm-long tapered slab waveguide in Fig. 4(b) uniformly distribute the point input beam to the grating layer. The width of each curved waveguide branch is 50 μm, the bending radius 0.5 mm and the spacing between the branches 0.8 mm as shown in the SEM image in Fig. 4(c). The dimensions of the grating cells and the image resolution are almost the same as those of the line beam type diffractive waveguide system.

When a single-mode fiber is connected to the sample as shown in Fig. 4(d), the seven designed images in Fig. 4(e)
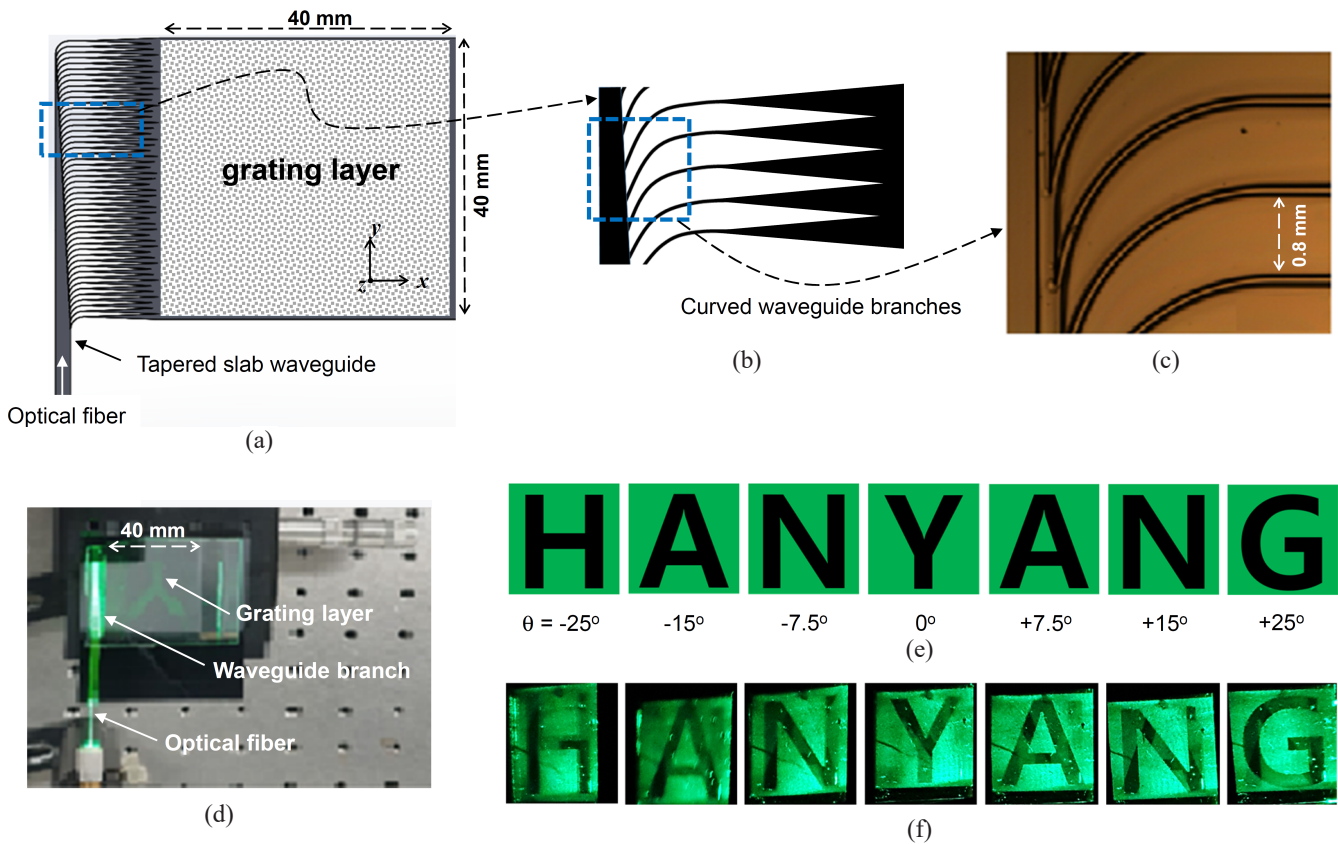
FIG. 4. Point source type setup for diffractive waveguide display. (a) Schematic diagram composed of a point source of optical fiber, tapered slab waveguide, curved waveguide branches, and grating layer on top of the planar waveguide. (b) and (c) are curved waveguide branches. (d) Measurement setup. (e) and (f) are designed images measured at seven multiple viewing angles in $\theta = -25°$ to $+25°$ from the normal direction of the grating layer.

are out-coupled from the grating layer and measured with distinguished viewing angles from $-25°$ to $+25°$ as shown in Fig. 4(f). The seven letters are clearly recognizable, but the image contrast and cross-talk noise might be slightly worse than those of the line beam type in Fig. 3. Larger negative viewing angles result in lower contrast due to the lower coupling efficiency of grating cells with smaller grating periods.

IV. CONCLUSION

We have demonstrated two types of light field displays based on diffractive waveguide configurations with a line beam incidence and a point source incidence, respectively. A 10 μm-square nanograting cell array, with periods of 300 nm–518 nm and slanted angles of $-8.5°\sim+8.5°$, were uniformly UV imprinted on the 40 mm × 40 mm surface of the slab waveguide to extract a set of seven images at different viewing angles. The integrated form of a point source type diffractive waveguide setup can also produce a set of images with well-distinguished light fields, similar to the case of a line beam type diffractive waveguide display. Even though the throughput efficiency from light source to camera detector could not be measured in the experiment, we expect that an out-coupling efficiency of 22.9% from

the grating cells after propagating a 40-mm-long diffractive waveguide can be achieved when the modulation depth of grating cells imprinted on the waveguide core is 120 nm. Further optimization of the thickness of the waveguide core and the grating fill factor will be helpful to improve the image uniformity and contrast visibility of very thin and flexible panels for multidirectional light field displays.

DISCLOSURES

The authors declare no conflicts of interest.

DATA AVAILABILITY

Data underlying the results presented in this paper are not publicly available at the time of publication, but may be obtained from the corresponding author upon request.

REFERENCES

1. J. Geng, "Three-dimensional display technologies," Adv. Opt. Photonics **5**, 456–535 (2013).

2. J. H. Han, J. Moon, D. H. Cho, J. W. Shin, C. W. Joo, J. Hwang, J. W. Huh, H. Y. Chu, and J. I. Lee, "Transparent OLED lighting panel design using two-dimensional OLED circuit modeling," ETRI J. **35**, 559–565 (2013).

3. J. Melzer and C. R. Spitzer, "Head-mounted displays," in *Digital Avionics Handbook*, 1st ed. (CRC press, USA, 2017), pp. 256–279.

4. Z. He, X. Sui, G. Jin, and L. Cao, "Progress in virtual reality and augmented reality based on holographic display," Appl. Opt. **58**, A74–A81 (2019).

5. Y. Wu, C. P. Chen, L. Mi, W. Zhang, J. Zhao, Y. Lu, W. Guo, B. Yu, Y. Li, and N. Maitlo, "Design of retinal-projection-based near-eye display with contact lens," Opt. Express **26**, 11553–11567 (2018).

6. E. Hua, W. Qiao, and L. Chen, "3D Holographic display with enlarged field of view based on binary optical elements," in *Proc. Progress in Electromagnetics Research Symposium* (*PIERS-Toyama*) (Toyama, Japan, Aug. 1–4, 2019), pp. 277–232.

7. J. Hua, E. Hua, F. Zhou, J. Shi, C. Wang, H. Duan, Y. Hu, W. Qiao, and L. Chen, "Foveated glasses-free 3D display with ultrawide field of view via a large-scale 2D-metagrating complex," Light Sci. Appl. **10**, 213 (2021).

8. Z. Huang, D. L. Marks, and D. R. Smith, "Out-of-plane computer-generated multicolor waveguide holography," Optica **6**, 119–124 (2019).

9. D. Fattal, Z. Peng, T. Tran, S. Vo, M. Fiorentino, J. Brug, and R. G Beasusoleil, "A multi-directional backlight for a wide-angle, glasses-free three-dimensional display," Nature **495**, 348–351 (2013).

10. F. Zhou, J. Hua, J. Shi, W. Qiao, and L. Chen, "Pixelated blazed gratings for high brightness multiview holographic 3D display," IEEE Photonics Technol. Lett. **32**, 283–286 (2020).

11. W. Wan, W. Qiao, W. Huang, M. Zhu, Z. Fang, D. Pu, Y. Ye, Y. Liu, and L. Chen, "Efficient fabrication method of nano-grating for 3D holographic display with full parallax views," Opt. Express **24**, 6203–6212 (2016).

12. J.-L. Feng, Y.-J. Wang, S.-Y. Liu, D.-C. Hu, and J.-G. Lu, "Three-dimensional display with directional beam splitter array," Opt. Express **25**, 1564–1572 (2017).

13. M. Khorasaninejad, W. Chen, R. C. Devlin, J. Oh, A. Y. Zhu, and F. Capasso, "Metalenses at visible wavelengths: Diffraction-limited focusing and subwavelength resolution imaging," Science **352**, 1190–1194 (2016).

14. Y. Su, Z. Cai, K. Wu, L. Shi, F. Zhou, H. Chen, and J. Wu, "Projection-type multi-view holographic three-dimensional display using a single spatial light modulator and a directional diffractive device," IEEE Photonics J. **10**, 7000512 (2018).

15. W. Wan, W. Qiao, W. Huang, M. Zhu, Y. Ye, X. Chen, and L. Chen, "Multiview holographic 3D dynamic display by combining a nano-grating patterned phase plate and LCD," Opt. Express **25**, 1114–1122 (2017).

16. D. Cheng, Y. Wang, C. Xu, W. Song, and G. Jin, "Design of an ultra-thin near-eye display with geometrical waveguide and freeform optics," Opt. Express **22**, 20705–20719 (2014).

17. C. Yu, Y. Peng, Q. Zhao, H. Li, and X. Liu, "Highly efficient waveguide display with space-variant volume holographic gratings," Appl. Opt. **56**, 9390–9397 (2017).

18. N, Zhang, J, Liu, J, Han, X, Li, F, Yang, X, Wang, B, Hu, and Y. Wang, "Improved holographic waveguide display system," Appl. Opt. **54**, 3645–3649 (2015).

19. S. Park, B. J. Park, S. Yun, S. Nam, S. K. Park, K. and U. Kyung, "Thin film display based on polymer waveguides," Opt. Express **22**, 23433–23438 (2014).